INTERNATIONAL INSTITUTE OF WELDING
A world of joining experience

COMMISSION XV

DESIGN,

ANALYSIS AND

FABRICATION OF WELDED STRUCTURES

XV-1409-12, XV-F-88-12

SEISMIC DESIGN OF A V-BRACED 3D MULTI-STORY STEEL FRAME

Author(s) József Farkas, Károly Jármai

Abstract:

The seismic design process is detailed for a spatial V-braced three-bay three-story steel frame. In the case of a 3D frame, the seismic forces should be multiplied by a factor prescribed in Eurocode 8. In this way, the spatial frame can be regarded as a plan one. The V-bracing rods of circular hollow section (CHS) should absorb the seismic energy, but their overall buckling resistance should be smaller than the seismic rod force. The interstory drift is so small that the braced frame can be designed as a non-sway one. The beams of rolled UB profile are designed for normal force and bending moment, including the effect of the unbalanced force due to the buckling of braces. The columns of CHS profile are designed for compression force. The design of a bolted beam-to-column connection and a bolted joint of a brace is also treated. MathCAD algorithms are used to fulfil the design constraints.

IIW Keywords: braced steel frames, seismic design of frames, seismic energy absorption by buckling, bolted joints

Date of creation: 19.06.2012 – Last saved on 19/06/2012 14:32:00 (rev.2)

Seismic design of a V-braced 3D multi-story steel frame

Author(s) József Farkas, Károly Jármai

Author information József Farkas[1], Károly Jármai[2] University of Miskolc, H-3515 Miskolc, Hungary [1]Professor emeritus, Dr.sci.techn. altfar@uni-miskolc.hu [2]Professor, Dr.sci.techn. altjar@uni-miskolc.hu

ABSTRACT

The seismic design process is detailed for a spatial V-braced three-bay three-story steel frame. In the case of a 3D frame, the seismic forces should be multiplied by a factor prescribed in Eurocode 8. In this way, the spatial frame can be regarded as a plan one. The V-bracing rods of circular hollow section (CHS) should absorb the seismic energy, but their overall buckling resistance should be smaller than the seismic rod force. The interstory drift is so small that the braced frame can be designed as a non-sway one. The beams of rolled UB profile are designed for normal force and bending moment, including the effect of the unbalanced force due to the buckling of braces. The columns of CHS profile are designed for compression force. The design of a bolted beam-to-column connection and a bolted joint of a brace is also treated. MathCAD algorithms are used to fulfil the design constraints.

IIW-Thesaurus keywords braced steel frames, seismic design of frames, seismic energy absorption by buckling, bolted joints:

1 Introduction

The aim of the present study is to show by a numerical problem the seismic design process of a spatial steel frame including the effect of concentric V-bracings. In the design of braces the energy absorbing capacity is also considered using the developed own formulae.

In the design of braces, beams and columns MathCAD algorithms are used in order to exactly fulfil the constraints, i.e. to obtain the most economic structure. The rules of Eurocodes 3 and 8 are applied. Circular hollow sections are used for braces and columns and rolled UB profiles are applied for beams.

The design of the 3D frame is reduced to a planar one multiplying the seismic forces by a factor of 1.3. The beams and columns are designed as parts of a non-sway frame. The braces are designed to allow the overall buckling and to absorbing the seismic energy. In the design of beams the unbalanced force due to buckling of the compression brace is also considered.

The beams are subject to compression and bending and the columns are loaded by compression. In the design of beams and columns the actions due to seismic forces should be multiplied by a factor of 1.25. The design of beam-to-columns connections and the joints of braces is included.

A brief literature survey of V-braced steel frames is given as follows.

Medhekar and Kennedy [1,2] have investigated the seismic design of a concentrically braces single- and two-storey building using hollow section braces and W-section columns.

Mualla and Belev [3] have shown a new friction damper device used for V-bracing.

Moghaddam et al. [4] have treated the design of concentrically braced steel frames. The cross sections of beams and columns were unchanged during the optimization process and the braces have been designed to minimize the story drift.

Longo et al. [5] have designed a V-braced 3 bay 4 story 3D building frame. HE European wide flange beam profiles have been used.

Ragni et al. [6] have proposed analytical expressions for dissipative bracings and used them for the design of 5-bay 4- and 8-storey frames.

Roeder et al. [7] have elaborated a simple design procedure for concentrically braced gusset plate connections considering the yield mechanism of such joints. In the appendix a detailed numerical example is given.

The design steps of the present study are as follows.

1. Main dimensions of the given frame
2. Calculation of non-seismic and seismic loads
3. Design of circular hollow section (CHS) V-bracings
4. Design of rolled I-section beams
5. Design of CHS columns
6. Design of the beam-to-column connections and joints of braces

1. Main dimensions of the given frame

The investigated frame is 3D symmetric in plan, three-bay three-story frame with V-bracings (Figure 1).

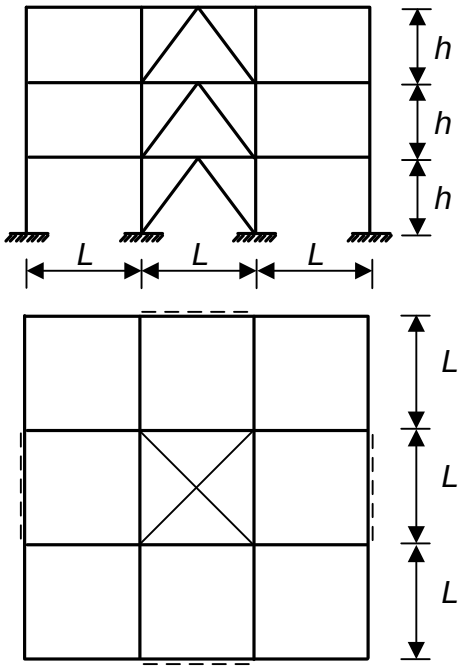

Figure 1. Elevation and ground-plan of the investigated frame. V-bracings are used in the outer plans, the central field is not loaded. *L* = 6 m, *h* = 3.6 m

2. Loads

2.1. Vertical loads

Dead load (G): roof 5.5 kN/m^2, floors 5.0 kN/m^2, live load (Q) 2.0 kN/m^2,

$$G+\psi Q, \psi = \varphi\psi_2, \psi_2 = 0.3, \text{ for roof } \varphi_1 = 1, \text{ for floors } \varphi_2 = 0.5.$$

Roof: 5.5 + 0.3x2 = 6.1 kN/m^2, floors: 5+ 0.15x2 = 5.3 kN/m^2.

For the whole area of 8x6x6 = 288 m^2 and for all storeys

W = 6.1x288 + 2x5.3x288 = 4809.6 kN.

2.2. Seismic load

According to Eurocode 8 the horizontal seismic force can be calculated as

$$F_b = S_d(T_1)m\lambda\,. \tag{1}$$

For a centrally braced frame of height 3x3.6 = 10.8 m

$$T_1 = 0.050x10.8^{0.75} = 0.298, q = 2.5. \tag{2}$$

For a subsoil of class C S = 1.15, T_B = 0.2, T_C = 0.6, T_D = 2.

For $T_B < T_1 < T_C$, calculating with a_g = 0.4 m/s^2,

$$S_d = a_g Sx2.5/q = 0.4x1.15 = 0.46 \text{ and } \lambda = 0.85, \tag{3}$$

$$F_b = 0.46x0.85x4809.6 = 1880 \text{ kN.}$$

Distribution of the seismic force for roof and floors

$$F_i = \frac{z_i W_i}{\sum_i z_i W_i}, \tag{4}$$

$$\sum_i z_i W_i = 3.6x288(3x6.1 + 2x5.3 + 5.3) = 35458 \text{ kNm},$$

$$F_{roof} = 1880\frac{3.6x3x6.1x288}{35458} = 1006 \text{ kN},$$

$$F_{floor2} = 1880\frac{2x3.6x5.3x288}{35458} = 583 \text{ kN},$$

$$F_{floor1} = 1880\frac{3.6x5.3x288}{35458} = 291 \text{ kN.}$$

These horizontal seismic forces should be multiplied by 1.3 for the symmetric 3D frame and divided by 2 for a braced plane. Thus, for a braced plane the following horizontal seismic forces are acting (Figure 2): F_1 = 654, F_2 = 379, F_3 = 189 kN.

3. Design of CHS V-bracings

3.1. Constraint on tensile stress

$$S_b \le A_b f_y, f_y = 235 \text{ kN}, \tag{5}$$

where

$$S_b = Fs / L\,, \tag{6}$$

is the tensile/compression force in a brace, *F* is the sum of horizontal seismic forces acting above the brace.

3.2. Constraint on overall buckling

$$S_{cr} = \chi A_b f_y \le S_b\,,\quad \chi = \frac{1}{\phi + \sqrt{\phi^2 - \bar{\lambda}^2}}\,, \tag{7}$$

since the compression brace should buckle to absorb the seismic energy.

$$\phi = 0.5\left[1 + \alpha\left(\bar{\lambda} - 0.2\right) + \bar{\lambda}^2\right], \alpha = 0.34\,, \tag{8}$$

$$\lambda = \frac{ks}{r}, s = \sqrt{h^2 + \left(\frac{L}{2}\right)^2}\,, \tag{9}$$

k = 0.7 for 1b brace, *k* = 1 for 2b and 3b braces (see Fig. 6),

$$\bar{\lambda} = \frac{\lambda}{\lambda_E}, \lambda_E = \pi\sqrt{\frac{E}{f_y}}\,. \tag{10}$$

3.3. Constraint on strut slenderness for seismic zone

$$\lambda \le 80\,. \tag{11}$$

3.4. Absorbed energy of CHS and SHS braces cyclically loaded in tension-compression

Braces play an important role in the earthquake-resistant design of frames. The efficiency of bracing is characterized by the absorbed energy which can be obtained as the area of the hysteretic loop.

Studies have shown that the first critical overall buckling strength decreases during the second and third cycle, but after a few cycles, the hysteretic loop becomes stable. This degradation is caused by the Bauschinger-effect and by the effect of residual camber as explained by Popov and Black [8]. Unfortunately, these effects cannot be considered by analytical derivations; thus, the characteristics of the stable hysteretic loop will be taken from the experimental data published in the literature.

The aim is to derive simple closed formulae for the calculation of the area of the stable hysteretic loop. The derived formulae enable designers to analyze the effect of some critical parameters such as the yield stress of steel, end restraint and cross-sectional shape, and to work out aspects of optimization, i.e. the increasing of the energy-absorbing capacity of braces.

The stable hysteretic loop is shown schematically in Fig.1. The characteristics obtained by experiments are summarized in Table 1. It can be seen that, for η and z_1 the approximate value of 0.5 is predominantly obtained. The sum of relative axial shortenings $x + |x_1|$ varies in range of 5 - 14. On the basis of these data we consider the values $\eta = z_1 = 0.5$ and $x_0 = 1$, $x_1 = -5$.

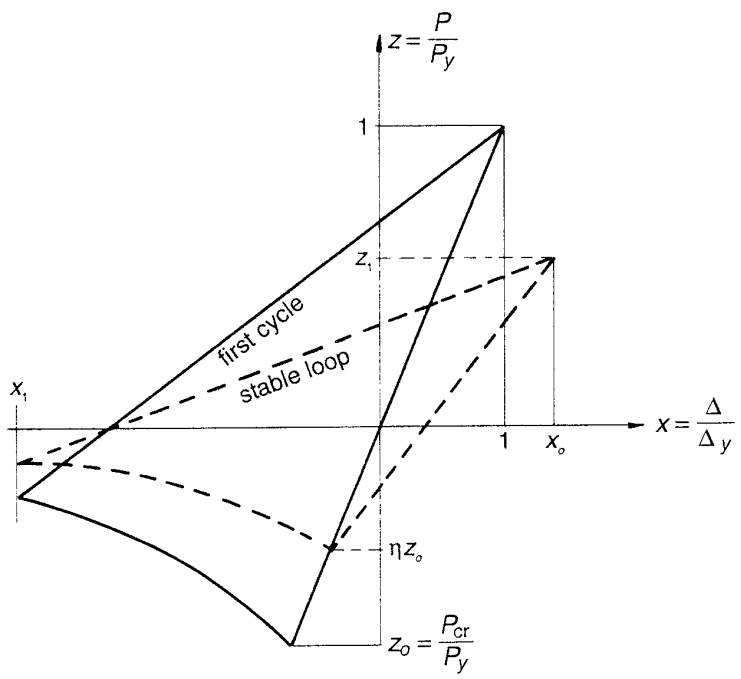

Figure 2. Characteristics of a stable hysteretic loop

Table 1 Characteristics of the stable hysteretic loop according to Fig.2.

Reference	x_0	x_1	η	z_1	cross-section
Jain [9]	2	-12	0.5	1	SHS
Liu [10]	2	-10	0.5	0.5	RHS
Matsumoto [11]	2	-10	0.5	0.5	CHS
Nonaka [12]	4	-4	0.5	0.8	Solid square
Ochi [13]	1	-10	0.5	0.5	CHS
Papadrakakis [14]	1	-4	0.5	0.5	CHS
Prathuangsit [15]	1	-12	0.5	0.5	I
Shibata [16]	5	-5	0.5	0.5	I

Another fundamental problem is the local buckling. According to many authors, e.g. Lee and Goel [17], it is recommended to avoid local buckling. Unfortunately, one can find extremely few proposed values for the limiting *D/t* or *b/t* ratios, in the case of cyclic plastic stress. For CHS Zayas et al. [18] proposed

$(D/t)_L$ = 6820/f_y where f_y is the yield stress in MPa, thus, for yield stress of 235 and 355 MPa one obtains 29 and 20, respectively.

For SHS or RHS Liu and Goel [10] proposed $(b/t)_L$ = 14 for f_y = 371 MPa, thus, we take for 355 MPa the value of 15 and for 235 MPa $15(355/235)^{0.5}$ = 19.

The limitation of the strut slenderness plays also an important role. API [19] proposed *KL/r*<80 (Eq. 11).

The relationship axial force - axial shortening $(P-\Delta)$ (Fig.3) has been derived for CHS struts by Supple and Collins [20] using the simple plastic hinge method:

The bending moment at the middle of the rod is $M = a_o P$, thus $a_0 = M/P$. The plastic axial shortening is caused by curvature, so (Fig.3)

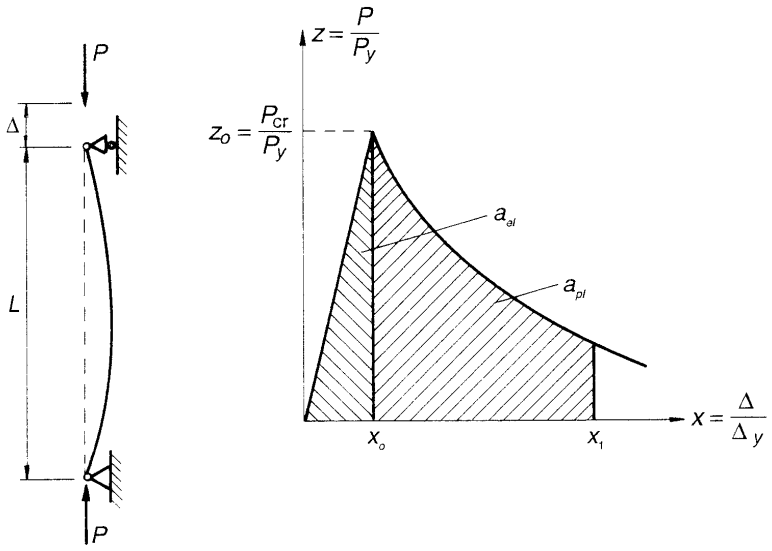

Figure 3. Post-buckling behaviour and the related specific areas

$$\Delta_{pl} = \int_0^L (ds - dx) \cong \frac{1}{2}\int_0^L \left(\frac{dy}{dx}\right)^2 dx \quad \text{since} \quad \frac{ds}{dx} = \sqrt{\left(\frac{dy}{dx}\right)^2 + 1} \approx 1 + \frac{1}{2}\left(\frac{dy}{dx}\right)^2 \quad (12)$$

Taking $y = a_0 \sin(\pi x / L)$ we obtain

$$\Delta_{pl} = \frac{1}{2}\int_0^L \frac{\pi^2 a_0^2}{L^2} \cos^2 \frac{\pi x}{L} dx = \frac{\pi^2 a_0^2}{4L} = \frac{\pi^2}{4L}\left(\frac{M}{P}\right)^2. \quad (13)$$

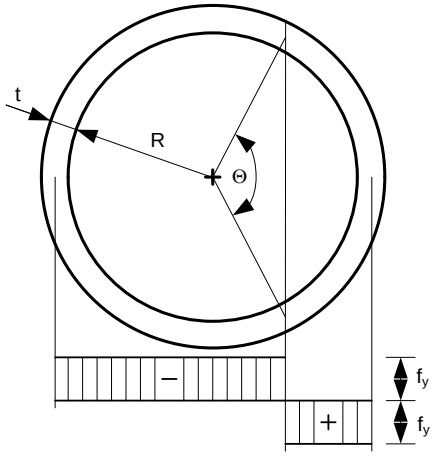

Figure 4. Plastic stress distribution

The squash load is $P_y = 2R\pi t f_y$. The plastic stress distribution shown in Fig.4 can be divided into two parts, one of them is caused by the compressive force, the second is caused by the bending moment. The plastic compressive force is

$$P = 2 f_y R\pi t - 2 f_y R\Theta = P_y\left(1 - \frac{\Theta}{\pi}\right), \tag{14}$$

from which

$$\frac{\Theta}{2} = \frac{\pi}{2} - \frac{\pi P}{2P_y}. \tag{14a}$$

The bending moment of the plastic zone is

$$M = 2\int_0^{\Theta/2} R\cos\varphi(2 f_y t R d\varphi) = 4 f_y R^2 t \sin\frac{\Theta}{2}. \tag{15}$$

where

$$\sin\frac{\Theta}{2} = \cos\left(\frac{\pi P}{2P_y}\right). \tag{15a}$$

Thus, $$\Delta_{pl} = \frac{D^2}{4L}\left[\frac{P_y}{P}\cos\left(\frac{\pi P}{2P_y}\right)\right]^2, \tag{16}$$

and

$$\Delta = \Delta_{el} + \Delta_{pl} = \frac{PL}{AE} + \frac{\alpha D^2}{4L}\left[\frac{P_y}{P}\cos\left(\frac{\pi P}{2P_y}\right)\right]^2, \tag{16a}$$

where α is the end restraint factor, for pinned ends $\alpha = 1$, for fixed ends $\alpha = 4$.

Using notations $x = \Delta / \Delta_y$, $z=P/P_y$, $z_o=P_{cr}/P_y$, $x_0 = \Delta_{el} / \Delta_y = P_{cr} / P_y = z_0$ Eq.(16) can be written in the form

$$x - x_0 = C_1\left[\frac{\cos^2(\pi z/2)}{z^2} - C_2\right]; \quad C_1 = \frac{\alpha D^2 E}{4L^2 f_y}: \quad C_2 = \frac{\cos^2(\pi z_0/2)}{z_0^2}. \tag{17}$$

For z<0.4 the following approximation is acceptable

$$\cos(\pi z/2) \approx 1 - \pi^2 z^2/8 \quad \text{and} \quad \cos^2(\pi z/2) \approx 1 - \pi^2 z^2/4. \tag{18}$$

and Eq.(17) takes the form

$$x - x_0 = C_1\left(\frac{1}{z^2} - \frac{\pi^2}{4} - C_2\right), \tag{19}$$

from which one obtains

$$z = C_1^{1/2}\left(x - x_0 + \frac{C_1\pi^2}{4} + C_1C_2\right)^{-1/2}. \tag{20}$$

The areas shown in Fig.3 can be calculated as follows:

$$a_{el} = z_0^2/2, \tag{21}$$

and

$$a_{pl} = \int_{x_0}^{x_1} z\,dx = 2C_1^{1/2}\left[\left(x_1 - x_0 + \frac{C_1\pi^2}{4} + C_1C_2\right)^{1/2} - \left(\frac{C_1\pi^2}{4} + C_1C_2\right)^{1/2}\right]. \tag{22}$$

It is possible to derive similar formulae for SHS struts. The results are as follows.

$$\Delta_{pl} = \frac{\alpha\pi^2}{4L}\left(\frac{M}{P}\right)^2 = \frac{\alpha\pi^2 b^2}{16L}\left(\frac{3}{4z} - z\right)^2, \tag{23}$$

and

$$x - x_0 = \frac{\Delta_{pl}}{\Delta_y} = C_3\left(\frac{3}{4z} - z\right)^2 + C_4; \quad C_3 = \frac{\alpha\pi^2 b^2}{16L^2 f_y}; \quad C_4 = C_3\left(\frac{3}{4z_0} - z_0\right)^2. \tag{24}$$

Expressing z from Eq.(13) we obtain

$$z = \frac{1}{2C_3^{1/2}}\left[\left(x - x_0 + 3C_3 + C_4\right)^{1/2} - \left(x - x_0 + C_4\right)^{1/2}\right], \tag{25}$$

and the area in the post-buckling range is

$$a_{pl} = \int_{x_0}^{x_1} z\,dx = \frac{1}{3C_3^{1/2}}\left[\left(x_1 - x_0 + 3C_3 + C_4\right)^{3/2} - \left(x_1 - x_0 + C_4\right)^{3/2} - \left(3C_3 + C_4\right)^{3/2} + C_4^{3/2}\right]. \tag{26}$$

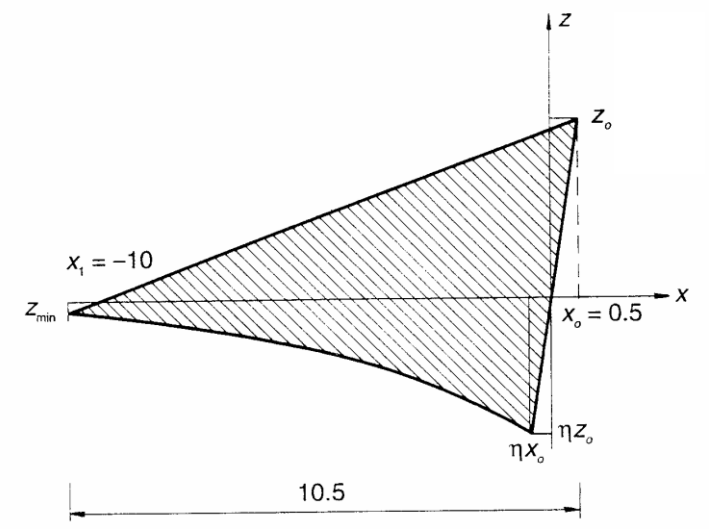

Figure 5. Area of the stable hysteretic loop

We consider the stable hysteretic loop according to Fig.5. The whole specific absorbed energy as the area shown in Fig.5 is

$$\sum_i a_i = a_{el} + a_{pl} + 10x0.5/2 - 10.5z_{\min}/2. \tag{27}$$

For a_{el} and a_{pl} we use Eqs(21),(22) or (26), but instead of $x_0=z_0$ we calculate with $\eta x_0 = \eta z_0, \eta = 0.5$. z_{min} is calculated using Eq.(20) or (25) taking x=10 and instead of x_0 taking $0.5x_0$.

The energy absorbing capacity of a strut is

$$F_{bo} = \left(\sum_i a_i\right) f_y A. \tag{27a}$$

3.5 Constraint on energy absorption capacity

$$S_b \le F_{br} = \left(\sum_i a_i\right) A_b f_y, \tag{28}$$

and Eqs (17), (21),(22), (27) are used.

The CHS dimensions are taken according to EN10210-2.

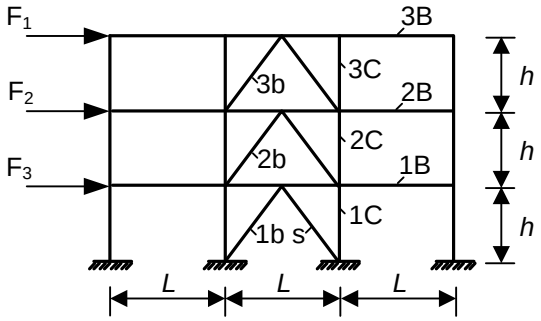

Figure 6. Horizontal seismic forces: F_1 = 654, F_2 = 379, F_3 = 189 kN. b - braces, B - beams, C – columns. $s = \sqrt{h^2 + (L/2)^2}$

3.6 Design results

Summary of the calculation results are given in Table 2.

Table 2. Characteristics of bracings. Dimensions in mm, forces in kN

Brace	F	S_b	Dxt	A_b mm^2	Tension Eq.(5)	λ Eq.(11)	S_{cr} Eq.(7)	F_{br} Eq.(12)
1b	1222	955	193.7x8	4670	1097	71.4	822	4647
2b	1033	807	177.8x8	4270	1003	71.4	709	3995
3b	654	511	177.8x5	2710	637	76.7	455	2558

It can be seen that the braces fulfil the constraints. F_{br} is much higher than F, since the decrease of the brace dimension is limited by the prescription of λ_{max} = 80.

Let us calculate the deformation of the compressed brace 3b during the overall buckling. Using Eq (16a)

$$\Delta = \Delta_{el} + \Delta_{pl} = \frac{S_{cr} s}{A_b E} + \frac{D^2}{4s}\left(\frac{S_y}{S_b}\cos\frac{\pi S_b}{2S_y}\right)^2 = \frac{455000x4686}{2710x2.1x10^5} + \frac{177.8^2}{4x4686}\left(\frac{637}{511}\cos\frac{\pi 511}{2x637}\right)^2, \quad (29)$$

$$\Delta = 2.15 + 0.24 = 2.39 \text{ mm}.$$

The interstory drift is the projection of the above value

$$\Delta_d = \Delta\frac{L}{2s} = 2.39\frac{3}{4.69} = 1.53 \text{ mm}. \quad (30)$$

This small value of the interstory drift shows that the braced frame can be designed as a non-sway one.

4. Design of beams

Beams of UB profile are designed according to Eurocode 8 [21] for vertical and seismic loads as members of a non-sway frame neglecting the support effect of bracings. The seismic forces are multiplied by 1.25.

Design of the beam 1B (Figure 6).

f_y = 335 MPa.

Compression force is

N = 1.25x1222 = 1528 kN.

Vertical load

p = 5.3x3 = 15.9 kN/m.

Bending moment from vertical load as a beam built-up at the ends

$M = pL^2/12$ = 71.55 kNm. (31)

According to Eurocode 8 [21] the beam should be designed also for the unbalanced force due to the overall buckling of the compression brace. For the beams built-up at the ends

$$V = Fh/L, M_V = VL/8. \quad (32)$$

Stress constraint for N and $M+M_V$ considering also the lateral torsional buckling

$$\frac{N}{\chi_y A f_y} + k_{yy}\frac{M+M_V}{\chi_{LT} W_y f_y} \le 1, \quad (33)$$

$$\frac{N}{\chi_z A f_y} + k_{zy}\frac{M+M_V}{W_y f_y} \le 1, k_{zy} = 0.8k_{yy}, \quad (34)$$

$$\lambda_i = \frac{L}{r_i}, \bar{\lambda}_i = \frac{\lambda_i}{\lambda_E}, i = y, z, \quad (35)$$

$$\chi_i = \frac{1}{\phi_i + \sqrt{\phi_i^2 - \bar{\lambda}_i^2}}, \quad (36)$$

$$\phi_i = 0.5\left[1 + \alpha_i\left(\bar{\lambda}_i - 0.2\right) + \bar{\lambda}_i^2\right], \alpha_y = 0.21, \alpha_z = 0.34, \quad (37)$$

$$k_{yy} = C_{my}\left(1 + 0.6\bar{\lambda}_y \frac{N}{\chi_y A f_y}\right), C_{my} = 0.95 \text{ if } \bar{\lambda}_y \le 1, \quad (38a)$$

$$k_{yy} = C_{my}\left(1 + 0.6\frac{N}{\chi_y A f_y}\right) \text{ if } \bar{\lambda}_y \ge 1, \quad (38b)$$

$$\chi_{LT} = \frac{1}{\phi_{LT} + \sqrt{\phi_{LT}^2 - 0.75\lambda_{LT}^2}}, \quad (39)$$

$$\phi_{LT} = 0.5\left[1 + \alpha_{LT}\left(\lambda_{LT} - 0.4\right) + 0.75\lambda_{LT}^2\right], \alpha_{LT} = 0.49, \quad (40)$$

$$\lambda_{LT} = \sqrt{\frac{W_y f_y}{M_{cr}}}, \quad M_{cr} = \frac{\pi^2 EI_z}{L^2}\sqrt{\frac{I_\omega}{I_z} + \frac{L^2 GI_t}{\pi^2 EI_z}}. \quad (41)$$

The results are summarized in Table 3.

Table 3. Characteristics of beams for braced fields. Stresses in MPa

brace	*N* (kN)	*p* (kN/m)	*V* (kN)	M_V (kNm)	Profile UB	Stress constraints Eq.(22) Eq.(23)
1B	1528	15.9	733.2	550	610x305x149	0.806<1, 0.758<1
2B	1291	15.9	621.0	466	610x229x140	0.903<1, 0.952<1
3B	818	18.3	392.4	294	610x229x101	0.938<1, 0.920<1

The beams fulfil the design constraints.

For the other non-braced fields, where $M_V = 0$ the following beam dimensions can be used (Table 4).

Table 4. Characteristics of beams for non-braced fields. Stresses in MPa

brace	*N* (kN)	*p* (kN/m)	*V* (kN)	M_V (kNm)	Profile UB	Stress constraints Eq.(22) Eq.(23)
1B	1528	15.9	733.2	0	610x229x125	0.35<1, 0.89<1
2B	1291	15.9	621.0	0	610x229x113	0.35<1, 0.86<1
3B	818	18.3	392.4	0	533x210x82	0.41<1, 0.94<1

5. Design of columns

Design of column 1C for overall buckling.

Compression force from horizontal seismic forces

$$N_h = 1.25x1033\frac{3.6}{6} = 775 \text{ kN.}$$

Compression force from vertical loads

$$N_v = 1.1\frac{(6.1+2x5.3)6^2}{2} = 331 \text{ kN.}$$

Total compression force

$$N = N_h + N_v = 1106 \text{ kN.}$$

The effect of bending moments can be neglected, since the inertia of columns is much less than that of beams.

Self masses of beams, columns and braces as additional loads for columns are also taken into account: for column 3C 8 kN, for 2C 21 kN and for 1C 37 kN.

The columns can be designed for compression force only. The calculations show that the bending moments can be neglected, since the ratio of moments of inertia of beams and columns is very small.

Overall buckling constraint (see Eqs 35, 36, 37)

$$\frac{N}{A} \le \chi f_y \text{ , } f_y = 235 \text{ MPa.} \qquad (42)$$

For the column 1C $k = 0.7$, for columns 2C and 3C $k = 1$.

Characteristics of CHS profiles are taken from EN 10210-2.

Design results are given in Table 5.

Table 5. Characteristics of CHS columns

Column	***N*** (kN)	CHS profile	A (mm^2)	r (mm)	Constraint Eq. (42) (MPa)
1C	1143	219.7x8	5310	74.7	215< 219
2C	737	193.7x8	4670	65.7	158< 198
3C	129	114.3x3.6	1250	39.2	103< 143

The column profiles fulfil the design constraints.

In order to show the economy of CHS profiles let us compare them with UC profiles. Since UC profiles are open sections, constraint on flexural-torsional buckling should also be taken into account with the following formulae (Farkas,J., Jármai,K. [22]).

$$\frac{N}{A} \le \chi_T f_y \text{ ,} \qquad (43)$$

$$\chi_T = \frac{1}{\phi_T + \sqrt{\phi^2 - \lambda_T^2}} \text{ , } \phi_T = 0.5\left[1 + \alpha_T(\lambda_T - 0.2) + \lambda_T^2\right] \text{ , } \alpha_T\, 0.49 \text{ ,} \qquad (44)$$

$$\lambda_T = \sqrt{\frac{f_y}{\sigma_{Tcr}}}, \quad \sigma_{Tcr} = \frac{\pi^2 EI_\omega}{h^2 I_p} + \frac{GI_t}{I_p}, \quad I_p = I_y + I_z. \tag{45}$$

The design results are given in Table 6. The overall flexural buckling constraint is checked according to formulae of Section 3.2 with respect to buckling around the axis *z*.

Table 6. Characteristics of UC columns. Stresses in MPa

Column	***N*** (kN)	UC profile	*A* (mm^2)	Constraint $N/A \le \chi_z f_y$	Constraint $N/A \le \chi_T f_y$
1C	1143	203x203x52	6628	172<195	172<190
2C	737	203x203x46	5873	125<163	125<185
3C	129	152x152x23	2925	44<122	44<166

The comparison of cross-sectional areas in Tables 4 and 5 shows the economy of CHS profiles over UC sections. Disregarding the column 3C for which the minimal UC profile is used, mass savings about 20% can be achieved by using CHS profiles.

6. Design of joints

6.1. Beam-to-column connections

Let us check the bolts for 1B beam as shown in Figure 7.

It is supposed that the bending moment causes forces only in the bolts of flange splices.

The shear resistance of bolts M27 of grade 10.9 (ultimate tensile strength 1000 MPa) according Eurocode 3 Part 1-8 [23] is

$$F_R = \frac{2x0.5Af_{bu}}{\gamma_{M2}} = \frac{2x05x573x1000}{1.25x1000} = 458.4\,\text{kN}. \tag{46}$$

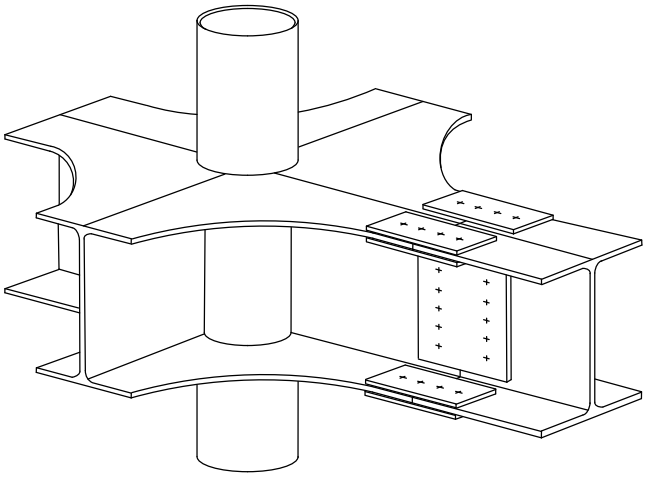

Figure 7. Beam-to-column connection

The forces in flange bolts caused by the bending moment M = 550 kNm are

F_{BM} = 550000/602.6 = 912.8 kN.

For one bolt F_{BM1} = 912.8/4 = 228.2 kN.

Forces in bolts from normal force N = 1532 kN F_{BN} = 1532/13 = 117.1 kN.

Force in flange bolts from M and N

F_f = 226.2 + 117.1 = 345.3 < 458.4 kN, OK.

The shear force in the connection from V and p

$$Q = \frac{V}{2} + \frac{pL}{2} = \frac{733.2}{2} + \frac{15.9x6}{2} = 366.6 + 47.7 = 414.3 \text{ kN.} \quad (47)$$

Force in one web bolt Q_W = 414.3/5 = 82.9 kN.

Shear force from N F_{BN} = 117.1 kN.

Shear force from Q und N in one web bolt

$$F_W = \sqrt{82.9^2 + 117.1^2} = 143.5 < 458.4 \text{ kN, OK.}$$

The connections of rolled UB profile beams and CHS columns can be realized as shown in Figure 7. The beams are connected by bolted splices to flange and web plates welded to the columns.

6.2. Joints of braces

The braces are connected to the columns and beams by bolted joints as shown in Figure 8 [24]

In the Figure 8. the following dimensions are applied. The normal force acting in the brace 1b is F = 955 kN. According to Eurocode 3 Part 1-8 [23] the load capacity of four M30 bolts of grade 10.9 with ultimate tensile strength of 1000 N/mm^2 is

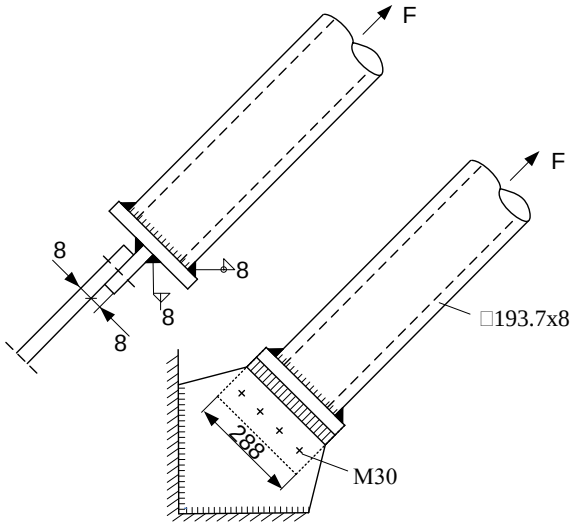

Figure 8. Bolted joint of a brace

$$F_V = \frac{4x0.5 f_{ub} A}{\gamma_{M2}} = \frac{4x0.5x1000x707}{1.25} = 1131 > 955 \text{ kN}. \quad (48)$$

The bearing resistance of 4 bolts for the plate thickness of t = 8 mm is

$$F_b = \frac{1.5 f_u dt}{\gamma_{M2}} 4 = \frac{1.5x1000x30x8x4}{1.25x1000} = 1152 > 955 \text{ kN}. \quad (49)$$

The load capacity of a = 8 mm size fillet welds is (for f_y = 235 MPa)

$$F_W = \frac{2a288 f_u}{1000\sqrt{3}\beta_W} = \frac{2x8x288x360}{1000\sqrt{3}x0.8} = 1197 > 955 \text{ kN}. \quad (50)$$

The load capacity of the a = 8 mm fillet weld connecting the CHS brace

$$F_{W1} = \frac{D\pi a f_u}{1000\sqrt{3}\beta_W} = \frac{193.7\pi 8x360}{1000\sqrt{3}x0.8} = 1265 > 955 \text{ kN}. \quad (51)$$

7. Conclusions

In the case of 3D frames the seismic forces should be multiplied by a factor prescribed by Eurocode 8. For frames of square symmetrical plans this factor is 1.3

The overall buckling resistance of V-bracings should be smaller than the rod force caused by seismic forces, but the energy absorption capacity of braces should be large enough.

The beams in the braced bay should be designed also for unbalanced vertical force due to buckling of compression braces. According to Eurocode 8, in the design of beams and columns the actions due to seismic forces should be multiplied by a factor of 1.25.

Since the interstory drift of braced frame is extremely small, it can be designed as a non-sway one.

The beams should be designed for compression force and bending moment including lateral- torsional buckling, while the columns are designed for overall buckling.

The columns are designed using also rolled UC profiles for comparison with CHS profiles. In this case the open UC profiles should be checked against flexural-torsional buckling. The comparison shows that mass savings of about 20% can be achieved by using CHS profiles instead of UC sections.

In the design of braces, beams and columns special MathCAD algorithms are used to achieve economy due to fulfilling the design constraints as most accurately as possible.

Acknowledgements

The research was supported by the Hungarian Scientific Research Fund OTKA T 75678 and by the TÁMOP 4.2.1.B-10/2/KONV-2010-0001 entitled "Increasing the quality of higher education through the development of research - development and innovation program at the University of Miskolc supported by the European Union, co-financed by the European Social Fund."

References

[1] Medhekar,M.S., Kennedy,D.J.L. Seismic evaluation of single-storey steel buildings. Can.J.Civ.Eng. 26: (1999) 379-394.

[2] Medhekar,M.S., Kennedy,D.J.L. Seismic response of two-storey buildings with concentrically braced steel frames. Can.J.Civ.Eng. 26: (1999) 497-509.

[3] Mualla,I.H. and Belev,B. Performance of steel frames with a new friction damper device under earthquake excitation. Engng Structures 24: (2002) 365-371.

[4] Moghaddam,H., Hajirasonliha,L. and Doostan,A. Optimum seismic design of concentrically braced steel frames: concepts and design procedures. J. Constructional Steel Research 61 (2005) No.2. 151-166.

[5] Longo,A., Montuori,R. and Piluso,V. Plastic design of seismic resistant V-braced frames. Journal of Earthquake Engineering 12: (2008) 1246-1266.

[6] Ragni,L., Zona,A. and Dall'Asta,A. Analytical expressions for preliminary design of dissipative bracing systems in steel frames. J. Constructional Steel Research 67: (2011) 102-113.

[7] Roeder,Ch.W., Lumpkin,E.J. and Lehman,D.E. A balanced design procedure for special concentrically braced frame connections. J. Construct. Steel Res. 67: (2011) 1760-1772.

[8] Popov EP, Black RG. Steel struts under severe cyclic loadings. *J.Struct.Div.Proc.ASCE,* 1981; **107:** 1857-1881.

[9] Jain AK, Goel SC, Hanson RD. Hysteretic cycles of axially loaded steel members. *J.Struct.Div.Proc.ASCE* 1980; **106:** 1777-1795.

[10] Liu Zh, Goel SC. Cyclic load behavior of concrete-filled tubular braces. *J.Struct.Eng.ASCE* 1988; **114:** 1488-1506.

[11] Matsumoto T, Yamashita M. et al. Post-buckling behavior of circular tube brace under cyclic loadings. *Safety Criteria in Design of Tubular Structures, Proc.Int.Meeting,* Tokyo,. Architectural Institute of Japan, 1987; 15-25.

[12] Nonaka T. Approximation of yield condition for the hysteretic behavior of a bar under repeated axial loading. *Int.J.Solids Struct*. 1977; **13:** 637-643.

[13] Ochi K,Yamashita M. et al. Local buckling and hysteretic behavior of circular tubular members under axial loads. *J.Struct.Constr.Engng AIJ* 1990; No.417: 53-61. (in Japanese).

[14] Papadrakakis M, Loukakis K. Elastic-plastic hysteretic behavior of struts with imperfections. *Eng.Struct*. 1987; **9:** 162-170.

[15] Prathuangsit D, Goel SC, Hanson RD. Axial hysteresis behavior with end restraints. *J.Struct.Div.Proc.ASCE*, 1978; **104:** 883-896.

[16] Shibata M. Analysis of elastic-plastic behavior of a steel brace subjected to repeated axial force. *Int.J. Solids Struct*. 1982; **18:** 217-228.

[17] Lee S, Goel SC. Seismic behaviour of hollow and concrete filled square tubular bracing members. *Research Report UMCE 87-11.* Department of Civil Engineering, University of Michigan, Ann Arbor, 1987.

[18] Zayas VA, Mahin SA, Popov EP. Ultimate strength of steel offshore structures. *Behaviour of offshore structures, Proc. 3rd Int. Conference*, Boston, Hemisphere Publ. Co,. Washington, Vol.2. 1982; 39-58.

[19] American Petroleum Institute (API) Draft Recommended Practice 2A-LRFD, first ed. 1989.

[20] Supple WJ, Collins I. Post-critical behaviour of tubular struts. *Eng.Struct*. 1980; **2:** 225-229.

[21] Eurocode 8: Design of structures for earthquake resistance. Part 1.: General rules, seismic actions and rules for buildings. EN 1998-1 (2008).

[22] Farkas,J., Jármai,K. Analysis and optimum design of metal structures. Rotterdam-Brookfield, Balkema, 1997.

[23] Eurocode 3 Part 1.8. Design of joints. EN 1993-1-8 (2002).

[24] Kurobane,Y. et al. Design guide for structural hollow section column connections. TÜV-Verlag, Köln, 2004.

About the authors József Farkas[1], Károly Jármai[2]
University of Miskolc, H-3515 Miskolc, Hungary
[1]Professor emeritus, Dr.sci.techn. altfar@uni-miskolc.hu [2]Professor, Dr.sci.techn. altjar@uni-miskolc.hu